Effect of Deposition Potential on the Mechanism and Corrosion Behavior of Zn-Fe-Co Thin Coatings Electrochemically Deposited on a Steel Substrate

Arafat Toghan[1,2,], M. M. Abou-krisha[1,2], F. H. Assaf [1], F. El-Sheref[1]*

[1] Chemistry Department, Faculty of Science, South Valley University, Qena 83523, Egypt
[2] Chemistry Department, College of Science, Imam Mohammad Ibn Saud Islamic University (IMSIU), Riyadh 11623, Saudi Arabia
[*]E-mail: arafat.toghan@yahoo.com

Herein, the effect of deposition voltage on the chemical composition, corrosion resistance, structure and surface properties of Zn-Fe-Co coatings was explored using potentiostatic measurements, cyclic voltammetry, linear sweep voltammetry, anodic linear polarization, atomic absorption spectroscopy, scanning electron microscope, and X- ray diffraction. The results indicated that the corrosion resistance is directly related to Co and Fe contents in Zn-Fe-Co deposits. A significant increase in the quantities, contents and efficiency of zinc was achieved by increasing the deposition voltage which led to a sharp decrease the polarization resistance of the coated alloys. This is due to the ease of dissolution of zinc compared to Co and Fe. Moreover, Zn-Fe-Co coatings with a high content of cobalt up to 37% possess superior corrosion resistance compared to the pure Zn coatings and Zn-Fe-Co coatings with low values of cobalt contents less than 6%. A mechanism for electrodeposition model has been proposed and discussed.

1. INTRODUCTION

The development and use of steel is witnessing a continuous technological revolution as it is used in many industrial applications as well as in construction and shipbuilding, cars, machines, equipment and others. However, as is well known, it faces a serious corrosion problem especially in an acidic environment. No one can deny the scientist's outstanding efforts to solve this problem a long time ago using many different techniques and possibilities. One possibility is to coat the steel surface

with a protective film using a variety of processes such as electroplating, magnetron sputtering, thermal spraying, pulse laser deposition, and chemical vapor deposition [1-7].

An alternative possibility is to use organic corrosion inhibitors [8-10]. Among all these technologies, electrochemical deposition is a highly effective method due to cost savings, energy saving, no need to use toxic reagents, and the thickness, structures, particle sizes and shapes of the deposited film that can be controlled by simply changing experimental conditions such as electroplating bath composition, temperature, concentration, deposition time, pH of solution as well as the applied voltage or current.

In particular, the electroplating of zinc-metal alloy on the steel surface has great benefits against corrosion problems [11-15]. Although the fabrication of zinc alloys with other metals, especially transition metals such as Ni, Cu, Fe, Mn, and Co can reduce the rate of dissolution of steel, but the corrosion stability and durability of these binary alloys is still insufficient to complete its protection. Recently, the incorporation of a third metal into the protective film to form triple alloys such as Zn-Ni-Co, Zn-Co-Fe, Zn-Ni-Mn and Zn-Fe-Co has significantly enhanced steel corrosion resistance [17-22]. It is well known that Zn-M alloys obey the abnormal codeposition type, preferring zinc deposition first because it is a less noble metal compared to other noble metals associated with the fabrication of alloys such as Cu, Ni, Co and Fe which may give them a unique characteristic, and therefore their alloys have attracted great interest recently.

Deposition potential is one of the most important variables in the electrochemical deposition process, which is directly related to economic efficiency, film properties as well as the chemical structure, composition, corrosion performance and alloy quality [23, 24]. From this standpoint, the present work aims to study the effect of setting the working electrode (steel substrate) at different constant deposition voltages in sulfate bath containing Zn^{2+}, Fe^{2+} and Co^{2+} species at room temperature. Based on the results obtained, the optimum range of deposition potentials that provide the best corrosion resistance for this type of alloy will be discussed on the steel substrate as well as electrodeposition mechanisms.

2. EXPERIMENTAL

All electrochemical experiments were conducted in a 100.0 cm³ electrochemical cell with a 3-electrodes set up. The working electrode (cathode) consists of a steel rod (type 9021I, 99.98% Fe) that has been mechanically machined and mounted in Teflon. Thus, only an area of 0.196 cm² cross-section is exposed to the experiment solution. This type has been used for potentiostatic current-time measurements, cyclic voltammetry (CV), anodic linear sweep voltammetry and anodic linear polarization experiments. Whereas, a 304 stainless-steel sheet (0.08% C, 17.5–20 % Cr, 8–11% Ni, 2% Mn, 1% Si, 0.045% P, 0.03% S, and balance Fe) has dimensions of 1.0 cm x 1.0 cm x 0.05 cm was used as a second type of working electrode for chemical analysis experiments of electrodeposited thin coatings, i.e. to determine the contents of Zn, Co and Fe. A platinum-rod (6.0 cm²) was used as an auxiliary electrode, and saturated calomel electrode (SCE) as a reference electrode.

All experiments have been carried out in duplicate and at 25°C and showed good reproducibility. For a standard bath deposition, a series of electrodeposition experiments on stainless steel sheets, at different duration were carried out and the relative standard deviation (RSD%) was found to be 2.5%, 4.3% and 3.2% for the Zn, Fe and Co contents in the deposit, respectively.

EG&G potentiostat\galvanostat (model 237A) controlled by a computer (using corrosion program 352) was used to perform all the experiments. Analar chemicals were used, without further refinement, to prepare all solutions using double distilled water. The electroplating sulfate bath, which is used for the preparation of Zn-Fe-Co thin Coatings on steel and stainless steel substrates, has a chemical composition: 0.20 M $FeSO_4$, 0.20 M $CoSO_4$, 0.20 M $ZnSO_4$, 0.20 M Na_2SO_4, 0.01 M H_2SO_4 and 0.20 M H_3BO_3 [15]. The pH of the solution was adjusted by adding few drops of dilute sulfuric acid until a pH of 2.5 was obtained [10]. To study the corrosion resistance of the electrically deposited Zn-Fe-Co layer on the steel surface, anodized linear polarization method (ALP), also called Tafel plot, was applied in 0.05 M HCl as a corrosive medium. The steel coated was washed with distilled water and then transferred to an electrochemical cell containing 100 cm^3 of 0.05 M HCl, accordingly. The corresponding electrochemical corrosion potential (E_{corr}) is therefore obtained for each thin coating (see Table 1).

Table 1. Electrochemical corrosion and chemical analysis parameters for Zn-Fe-Co thin coatings electrochemically coated on a steel substrate at room temperature using various deposition voltages.

Parameters	Deposition potential (V)					
	-1.0	-1.1	-1.2	-1.25	-1.3	-1.4
Zn mass (10^{-5} g)	10	84	136	199	294	448
Co mass (10^{-5} g)	12	10	11.4	15	22	28
Fe mass (10^{-5} g)	10	19.8	23.6	24.4	35.8	42
Thin coating total mass (10^{-5}g)	32	114	171	239	352	518
% Zn content	31.3	73.8	79.5	83. 5	83.6	86.5
% Co content	37.5	8.8	6.7	6.3	6.25	5.4
% Fe content	31.3	17.4	13.8	10.2	10.17	8.1
% E_{Zn}	24.6	59	44.6	28.4	27.1	21.3
% E_{Co}	32.8	7.8	4.2	2.4	2.3	1.5
% E_{Fe}	28.8	16.3	9.4	4.1	3.9	2.3
% $E_{Zn-Fe-Co}$	86	83.1	58.2	34.9	33.2	25.1
Thin coating thickness (μm)	0.20	0.78	1.17	1.64	2.4	3.56
E_{corr} (mV)	-447	-727	-996	-977	-973	-953
R_p (kΩ)	2.8	2.1	1.1	1.16	1.21	1.32

Furthermore, anodic linear stripping voltammetry (LSVs) was used to determine the phase structure of the electrochemically deposited Zn-Fe-Co thin coatings on steel surfaces at different

deposition potentials. The stripping voltammogram experiments were recorded in a solution containing 0.5 M Na_2SO_4 and 0.05 M EDTA. Using a slow sweep rate of 5 mV s^{-1}, a wide-range of anodic voltage from -1.2 to +0.4 V was applied (all vs. SCE) at room temperature. In order to obtain more information about the kinetics of electrochemical deposition/dissolution process, cyclic voltammetry (CV) was performed in a sulfate electroplating bath containing pure Zn^{2+}, pure Co^{2+}, pure Fe^{2+} and a combination of the three ions. CVs were performed in a potential window from + 0.4 to -1.3 V (vs. SCE) with a scan rate of 5 mV s^{-1} at room temperature.

Atomic Absorption Spectroscopy (AAS, Variian spectr AA 55) and Energy Dispersive X-ray Spectrometer (EDX, Isis® link software and X-ray detector 6587 model, Oxford, England) were used to analyze the electrochemically coated Zn-Fe-Co film on stainless-steel substrates, i.e. to determine the contents of Zn, Co and Fe. Therefore, for the analysis of AAS, the film was first washed with double distilled water, then left to dissolve in a beaker containing 50 cm^3 of HCl (20%). After confirming that it was completely dissolved, its contents were diluted with double distilled water in a 100 cm^3 volumetric flask. Thus, the total deposit mass, Zn %, Co %, Fe %, and current efficiencies and thickness of thin coatings were calculated [25]. A blank experiment was also performed as a preliminary step using a pure stainless steel substrate (i.e. without Zn-Fe-Co thin coating) immersed in a 20 % HCl solution. AAS analysis confirmed that there was no contribution of stainless steel to the content of Fe (Fe %). Scanning Electron Microscope (SEM, equipped with EDX, model JSM-5500 LV (JEOL, Japan) was used to inspect the surface morphology of coated thin coatings. The crystalline constituents as well as particle size of the coatings were analyzed by XRD model Bruker Axs-D8 Advance with Cu Ka radiation (k= 1.5406 A° and 40 mA).
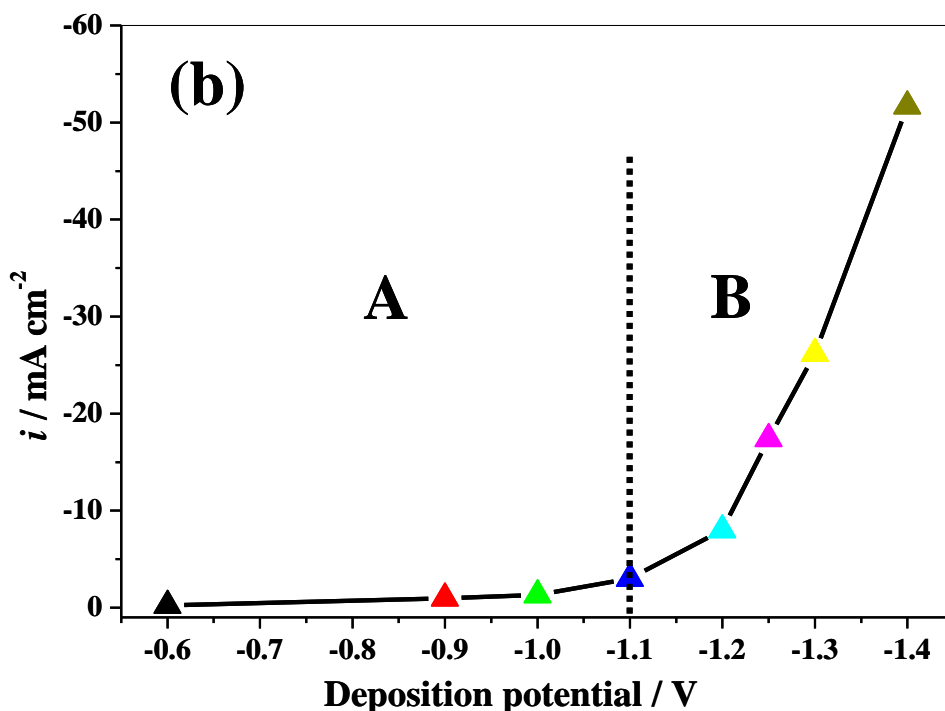
3. RESULTS AND DISCUSSION
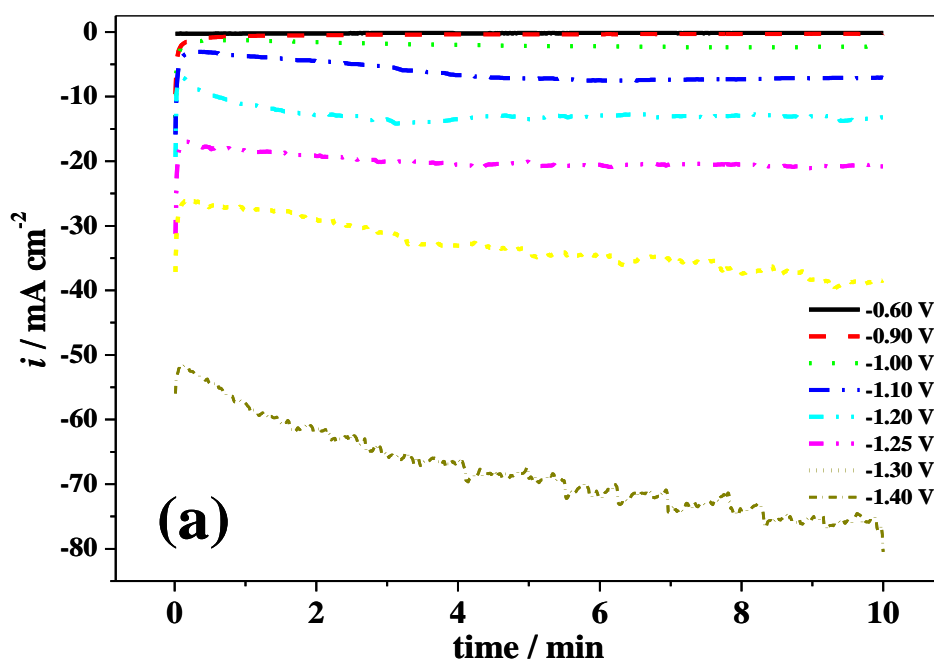
Figure 1. (a) Potentiostatic (i-t) curves obtained for a steel substrate immersed for 10 min at 25 °C in a standard sulfate electroplating bath (pH= 2.5) containing Zn^{2+}, Co^{2+} and Fe^{2+} species using different deposition potentials. (b) Relationship between changes in applied deposition potentials and their corresponding measured current densities (the data points were taken from Fig. 1a)

Figure 1a illustrates the potentiostatic current-time dependence recorded during the electrodeposition of the Zn-Fe-Co thin coating on the steel surface for 10 minutes with the change of deposition voltage (-0.6 to -1.4 V) and at 25°C. Interestingly, a sharp increase in current density occurred in only the first few seconds ($\approx$ 15 s) of deposition followed by a decrease. The initial increase of the current density is ascribed to the nucleation process, while the decrease is due to the diffusion process [26]. Thereafter, with the continued application of fixed voltage, a constant value of current density (i.e. steady state) was obtained in reference to the end of deposition. From this figure we can also observe that the increase in the deposition potential to more negative values leads to the flow of current density towards to more negative values, suggesting an increase in the deposition rate of Zn, Co and Fe. The initial nucleation growth step was observed in all deposition voltages to be examined except the -0.6 V. Surprisingly, although the initial steps of nuclei growth occurred during the first 15 seconds of applying voltages in the range from -1.1 to -1.4 V, current density fluctuations were measured. This is mainly attributed to the increase of the amount of Zn% in the deposit (see Table 1). Also, a wide gap in current density value was observed between the deposition potential at -1.3 and -1.4 V. This is due to an increase in hydrogen evolution reaction (HER) at -1.4 V as well as an increase in the deposition rate of all components (Zn, Co and Fe) [12]. Figure 1b displays the dependence of the current density (CD) increase on the applied potential. The CD first increases roughly slightly with the voltage before increasing sharply at -1.1 V. These results indicated that a

regular co-deposition of Zn-Fe-Co alloy (part A), i.e. cobalt and iron deposited preferentially compared to zinc, at potential < -1.1 V and abnormal co-deposition of Zn-Fe-Co (part B), i.e. preferential deposition of less noble metal zinc, at value > -1.1 V obtained [27].
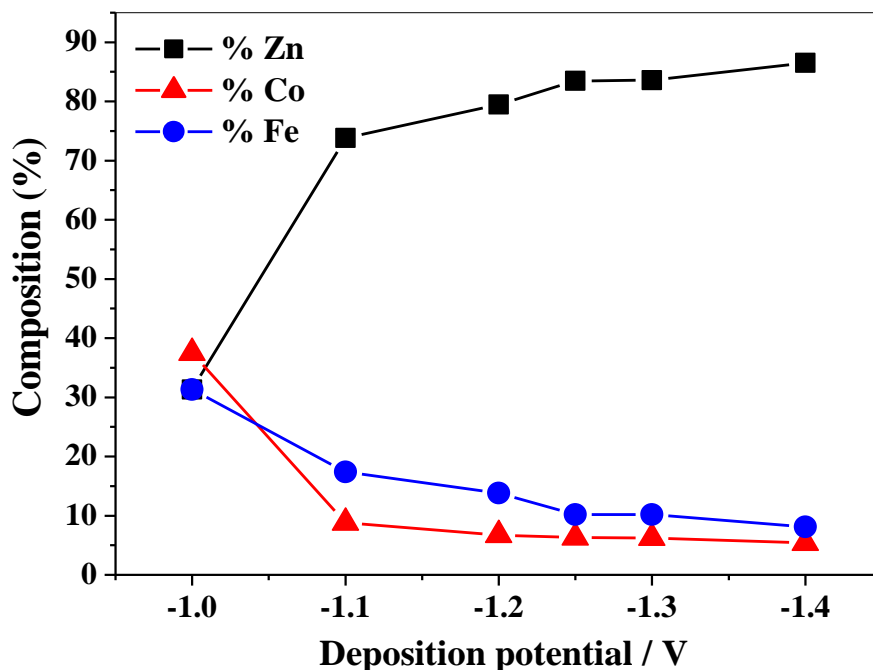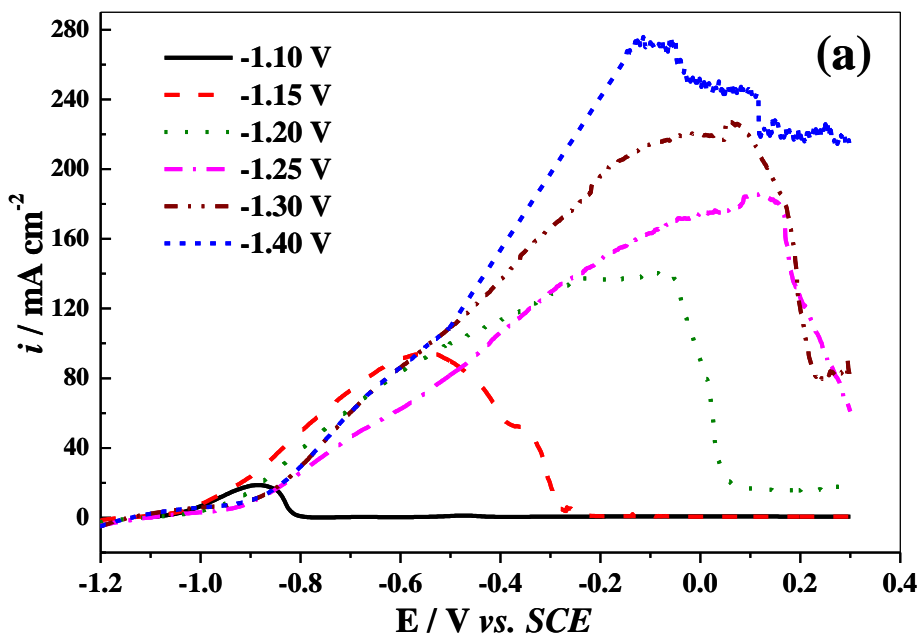

Figure 2. Effect of variation in applied deposition voltage on the composition of Zn-Fe-Co thin coatings.
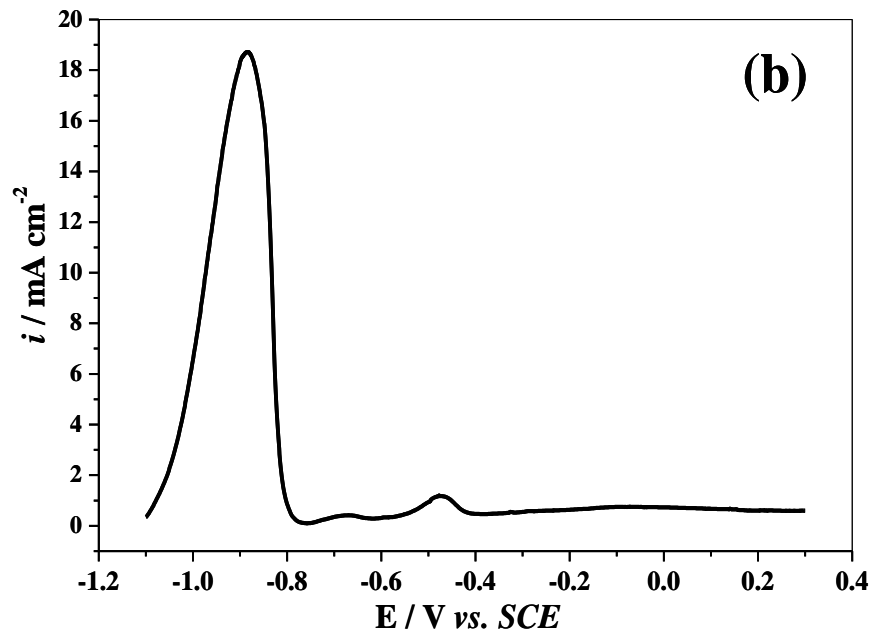
Figure 3. LSVs voltammograms obtained for Zn-Fe-Co thin coatings immersed in a mixture of 0.5 M Na$_2$SO$_4$ and 0.05 M EDTA using a sweep rate of 5 mV s^{-1} at 25 °C. Thin coatings were prepared on the surfaces of steel bars through the electrochemical deposition process as shown in Figure 1 by applying: (a) different deposition potentials, and (b) - 1.1 volts.

Noteworthy, at deposition voltages less than -1.1 volts, low overpotentials are needed to create the initial nucleus step for deposition of Co and Fe resulting in increased in their amounts, contents and current efficiencies of in deposits (see Table 1). In contrast, the favorable deposition of Zn requires higher nuclei over potentials, i.e. higher deposition voltages than -1.1 V, which increases the amount, content and current efficiency of zinc compared to the other two elements. The compositions of the electrochemically deposited Zn-Fe-Co coatings are displayed in Figure 2.

Figure 3 displays LSVs (anodic linear sweep voltammograms) measurements recorded during dissolution of the electrodeposited Zn-Fe-Co/steel thin coatings in a mixture of 0.5 M Na$_2$SO$_4$ and 0.05 M EDTA solution are presented. The choice of EDTA based on its ability to dissolve all alloy components as it is a powerful chelating agent [28,29]. In this way, LSVs (Figure 3a) is used precisely to explore the various phase structures of Zn-Fe-Co alloys that were electrochemically deposited on steel surfaces at different deposition voltages (-1.1 to -1.4 V). It can be seen that three different oxidation peaks (Figure 3b) were detected during dissolution of Zn-Fe-Co deposits and their intensity depends on the applied deposition potential. In conjunction with XRD patterns measured after different deposition potentials of Zn-Fe-Co alloys on steel plates, one can thoroughly examine the different structures of these thin solid thin coatings (see Figure 4). It noticed from this figure that all electrodeposited Zn-Fe-Co/steel thin coatings consist of pure zinc at the outer layer, pure Fe and CoFe phase formed near to the steel surface. Also, there are no phase's changes detected as a result of variation the deposition voltages. Figure 3b represents the dissolution of Zn-Fe-Co thin coating that was initially deposited at -1.1 V which shows three anodic peaks at -883, -680 and -471 mV. They correspond to the dissolution of Zn from the pure zinc phase, dissolution of Fe from pure iron and

FeCo phase, and the third anodic dissolution peak comes from the dissolution of Co from FeCo phase, respectively.
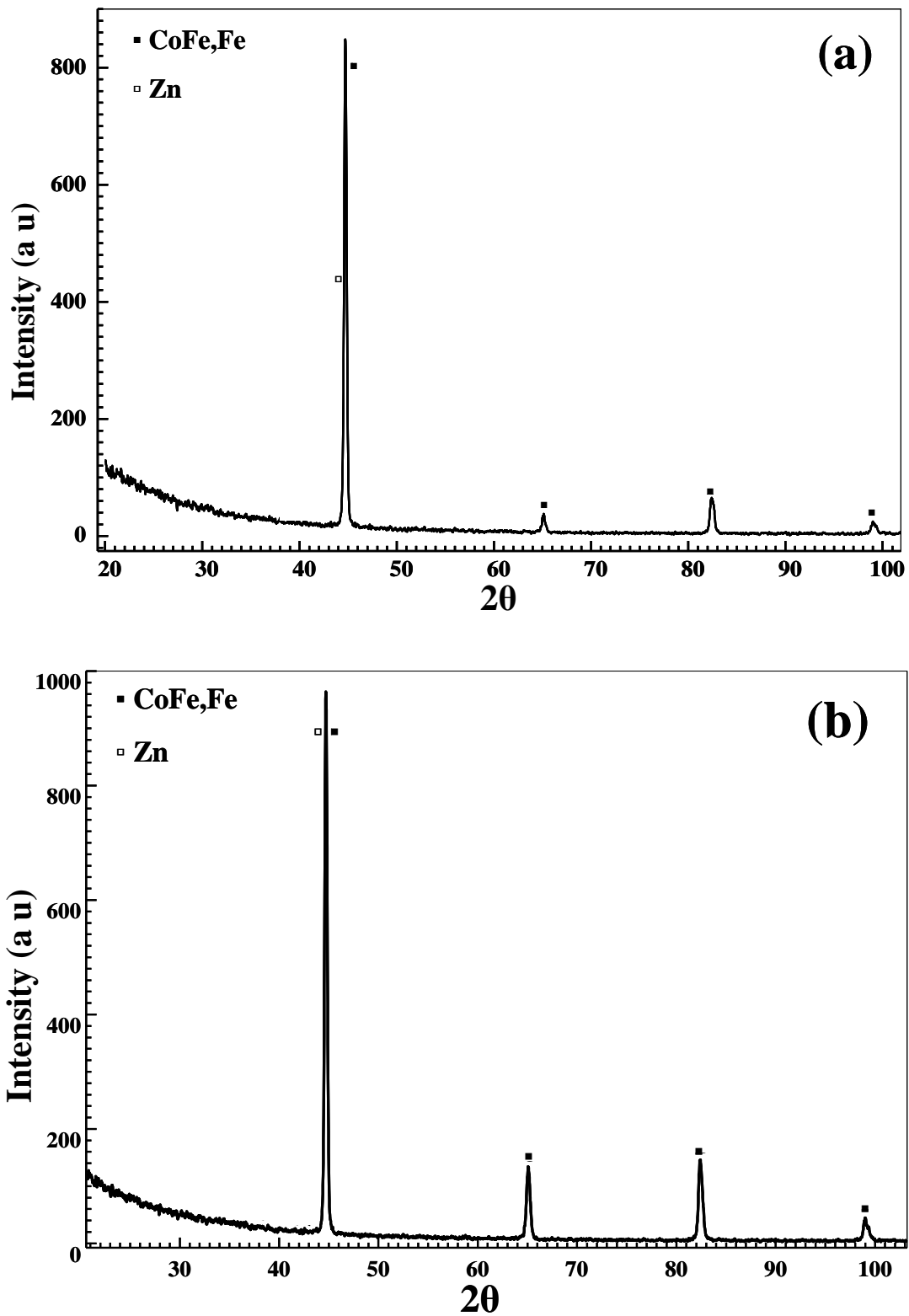

Figure 4. XRD patterns for Zn-Fe-Co alloys electrochemically deposited on steel sheets using different deposition potentials: (a) -1.1 V, and (b) -1.3 V.
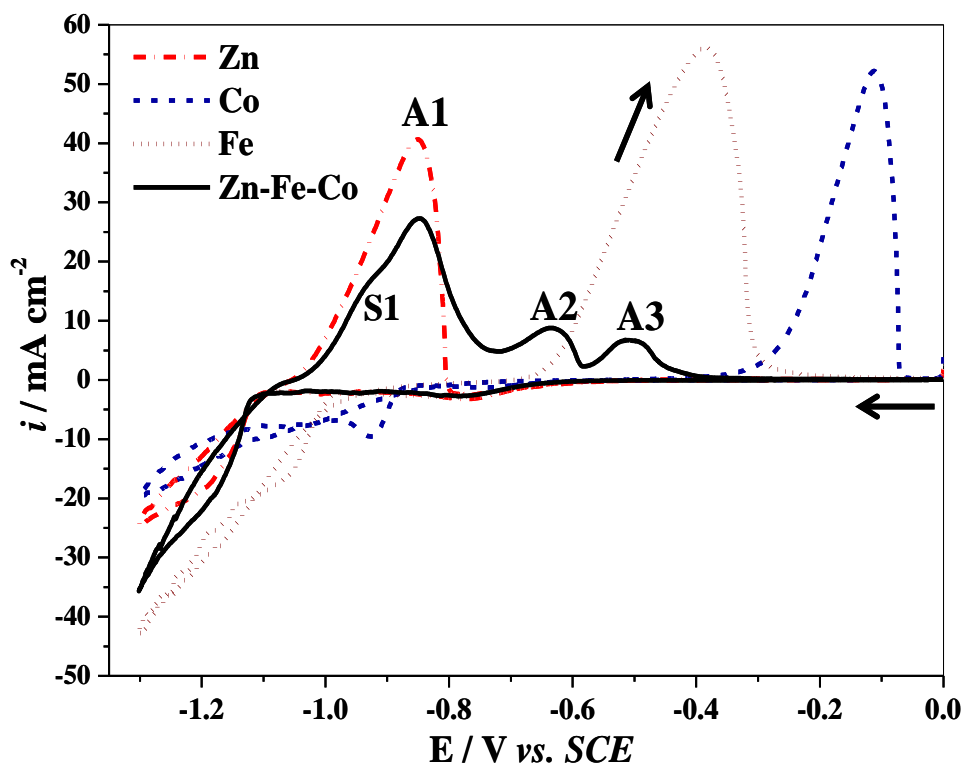
Figure 5. CVs curves recorded during the electrodeposition of pure Zn, pure Co, pure Fe and Zn-Fe-Co coatings on a steel substrate using sulfate bath with 0.01 M H_2SO_4, 0.20 M Na_2SO_4, 0.20 M H_3BO_3 and 0.20 M $ZnSO_4$ for pure Zn, 0.20 M $CoSO_4$ for pure Co, 0.2 M $FeSO_4$ for pure Fe or mix of 0.20 M $ZnSO_4$ + 0.20 M $CoSO_4$ + 0.20 M $FeSO_4$ for Zn-Fe-Co coatings with a scan rate of 5 mV s^{-1} at 25 °C.

Interestingly, on one hand the observed oxidation in peak dissolution height resulting from deposition at -1.1 V confirms the small amount of Zn, Co and Fe (see Table 1). On the other hand, there is a marked increase in the peak dissolution height when the deposition voltages increases (i.e. > -1.1 V) indicating an increase in the quantities of alloy components. Surprisingly, the current density did not reach a zero value at higher deposition potentials (from -1.2 to -1.4 V) indicating the incomplete stripping of the deposited thin coatings due to the significant increase in film thickness (see Table 1). Furthermore, peak distortions and fluctuations in the current values were observed with increase in deposition potential, which can be attributed to the increase of HER reaction during Zn-Fe-Co deposition resulting distortion of the deposited film (Figure 3a). In addition, the anodic peaks shift to a more positive direction, because of the increase in the amount of the nobler components of the alloy (i.e., Co and Fe) with increasing the deposition potential giving rise to more improvement of the corrosion resistance of the deposit.

Figure 5 shows a comparison between the CVs obtained during the deposition/dissolution of pure Zn, pure Fe, pure Co and Zn- Fe-Co coatings on the steel rod electrode. In the cathodic sweep, a reduction peak was observed during the electrochemical deposition of pure Co and pure Fe at potentials -870 and -970 mV; respectively, while, this peak was not seen the case of for pure Zn and Zn- Fe-Co coatings due to the interference between the deposition potential of zinc and its alloys with

HER reaction [21]. In the anodic scan, an anodic peak was observed at -850, -380 and -113 mV for dissolution of pure Zn, pure Fe, pure Co; respectively, while anodic dissolution of Zn-Fe-Co coating shows three oxidation peaks (A1-3) at -936, -634 and -502 mV and also a small shoulder at -844 mV. The first peak (A1) and the shoulder (S1) arise from the preferential dissolution of Zn from the pure Zn phase. The second peak (A2) resulting from the anodic dissolution of Fe from pure Fe and Fe from the FeCo structure formed near to the steel surface, while the third peak (A3) corresponds to the dissolution of Co from the FeCo phase. The height of A2 and A3 peaks is much smaller than A1, which can be expected because the contents of Fe and Co in Zn-Fe-Co coating alloys were very low under these conditions ($\approx$ 6 wt %). Also, obviously the anodic peaks that correspond to the dissolution of Fe and Co in the Zn-Fe-Co coating strongly turned into more negative potentials of about -250, -400 mV; respectively, compared to the anodic peaks in the case of pure Fe coating and pure Co coating as a result of formation of the FeCo phase.
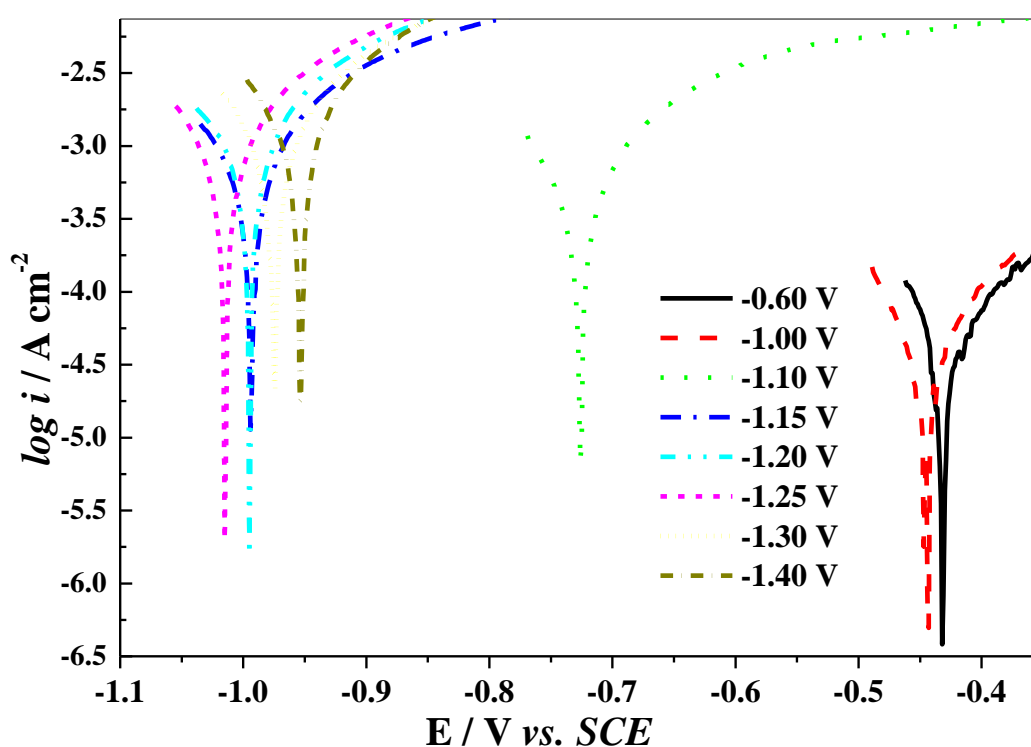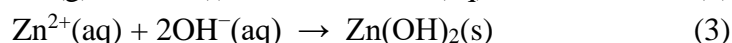

Figure 6. log i- E curves for Zn-Fe-Co thin coatings in a 0.05 M HCl solution at a scan rate of 25 mV s^{-1} and at 25 °C. Thin coatings were prepared on the surfaces of steel bars through the electrochemical deposition process by applying various static deposition voltages versus SCE as shown in Figure 1.

Tafel plots (log i-E curves) are used to study the corrosion resistance of the electrically deposited Zn-Fe-Co thin coatings on steel bars using different deposition voltages by stripping them anodicaly in a 0.05 M HCl solution at room temperature (see Figure 6). This can be achieved by determining the corrosion potential values (E_{corr}) for Zn-Fe-Co thin coatings prepared at different deposition voltages. The corrosion potential values of Zn-Fe-Co thin coatings are summarized also in

Table 1. It is clear from this figure that the corrosion potential values for thin coatings deposited at low deposition potentials of – 0.6 and -1.0 V, lie in the most positive direction at - 432.8 mV and - 447 mV, respectively, suggesting high corrosion resistance of these thin coatings due to high contents of noble metals (%Fe and %Co) in the deposit, i.e. normal co-deposition. Whereas, a remarkable shift in the corrosion potential value to a more negative direction (-996 mV) for Zn-Fe-Co thin coatings deposited at higher deposition voltages of -1.2 V, indicating switch from normal to abnormal co-deposition. Indeed, with abnormal codeposition the amount of zinc contents increases sharply, thus the polarization resistance decreases from 2.8 to 1.1 kΩ. The results also showed that the Zn-Fe-Co triple alloy coating which has a high cobalt ratio of up to 37% has superior corrosion resistance compared to a layer of pure Zn coating or from a triple alloy of Zn-Fe-Co containing a value less than 6% of cobalt as shown in Table 1.The results obtained here are fully consistent with previous work [18,30].

The question is what is the effect of applying very high deposition voltages (i.e. > -1.2 volts) on the polarization resistance of the Zn-Fe-Co composite thin coatings? One might expect a shift the E_{corr} of Zn-Fe-Co thin coatings deposited in very high deposition potentials to more negative and thus reduce the corresponding R_p values. The answer to this question was surprising as the corrosion potential values of the formed thin coatings at extremely high deposition voltages of -1.3 and -1.4 volts were again turned into less negative values of -975 and -952; respectively, indicating further polarization resistance and this is due to the significant increase in film thickness ($\approx$ 3.5 µm) as shown in Figure 6. Obviously, the polarization resistance of the Zn-Fe-Co thin coating depends not only on the amount of Co, Fe, or Zn in the film but also on the thickness of the film itself.

As we know, Zn deposition is preferably at high deposition voltage of -1.1 V (abnormal co-deposition) which of course leads to a sharp increase in its quantities and contents in electroplated Zn-Fe-Co thin coatings as well as an increase in film thickness (see Table 1). Accordingly, one would expect the polarization resistance of the thin coatings deposited using a very high deposition voltage (i.e. - 1.4 V) to be extremely high, as they have the highest thickness (3.56 µm), but because the dissolution of zinc from the deposits is also preferred than Co and Fe ((Eq. 1). Whereas, zinc content represents the highest percentage of alloys under these conditions (more than 80%). In this sense, a slight increase in polarization resistance was achieved from 1.1 to 1.32 kΩ with a significant increase in the deposition voltage from -1.2 to -1.4 volts, respectively. Therefore, when Zn-Fe-Co erodes, Zn begins to preferably dissolve first (anodic reaction) due to its high negative corrosion potential (Eq. 1). At the same time, the reduction of dissolved oxygen at the cathode occurs (Eq. 2). In this way, OH^- and Zn^{2+} ions are released while the film is corroding, which increases the local pH. Eventually, the dissolved Zn^{2+} reacts with OH^- species forming $Zn(OH)_2(s)$ which acts as a passive film on the surface of the eroded electrode as shown in Eq. 3 [23, 31]:

$$Zn(s) \rightarrow Zn^{2+}(aq) + 2e^- \tag{1}$$
$$O_2(g) + 2H_2O(l) + 4e^- \rightarrow 4OH^-(aq) \tag{2}$$
$$Zn^{2+}(aq) + 2OH^-(aq) \rightarrow Zn(OH)_2(s) \tag{3}$$

The effect of deposition potential on the microstructures of two Zn-Fe-Co alloys was examined by SEM as shown in Figure 7. The thin coatings were electrochemically deposited on steel plates by deposition voltages of -1.1 and -1.4 V for 10 minutes at 25ºC from the sulfate bath. A uniform, smooth, finer grain size and highly homogeneous film obtained at -1.1 V (Figure 7a), in contrast to

rough, non-uniform and inhomogeneous structure of the Zn-Fe-Co thin coating deposited at very high deposition potential of -1.4 V (Figure 7b). This is mainly due to an increase in the zinc content in the coating as well as the HER reaction, and therefore the film is distorted. In fact, the hydrogen evolution reaction has a strong impact on the nucleation process, the physical and structural properties of zinc coatings and this is due to the high reduction current required in the cathodic sweep process that makes it difficult to control the important properties of the formed film such as grain size, uniformity, adhesion, etc [32, 33].
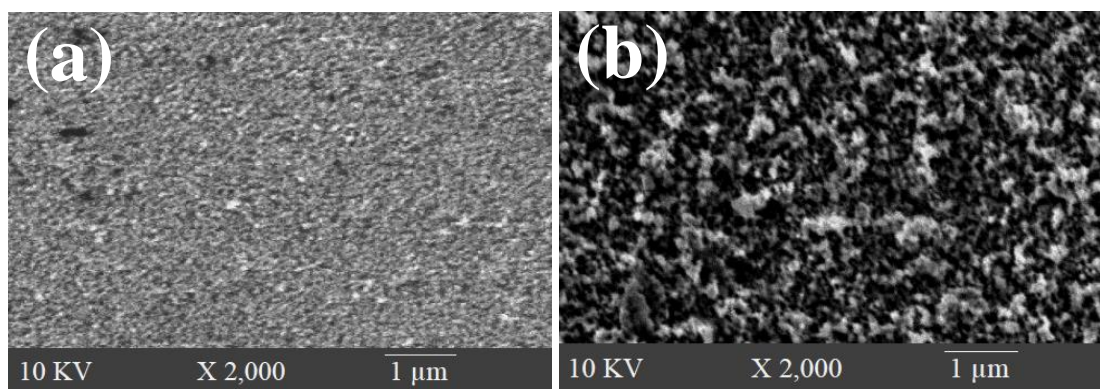

Figure 7. SEM micrographs for Zn-Fe-Co thin coatings electrochemically deposited on steel sheets for 10 min at 25 °C using different deposition potentials: (a) -1.1 V, and (b) -1.4 V.

Returning to the XRD patterns shown in Figure 4, the average particle size of Zn–Fe-Co thin coatings can be estimated using Debye-Scherrer equation [34]:

$$D = 0.9 \, \lambda \, / \, \beta \cos \theta$$

where λ, β, θ, and D refer to the X-ray wave length (0.1541 nm), full width at half maximum (FWHM), and diffraction angle and particle size; respectively. The grain size was calculated around the most intense peak. The estimated grain size of electrically deposited Zn-Fe-Co thin coatings on steel plates with a deposition voltage of -1.1 and -1.4 V for 10 minutes at room temperature from the sulfate bath was 68.8 and 170 nm, respectively. This finding confirms that the particle size in Zn-Fe-Co thin coatings has increased by increasing the deposition potential.

Inspection of the data summarized in Table 1, one can notice that the current efficiency (%E) of Zn, Fe and Co and Zn-Fe-Co alloy depends strongly on the applied fixed deposition potential. In fact, Zn^{2+} has deposition potential more negative compared to the potential for hydrogen evolution reaction, thus H_2 evolution is always in a competition with the alloy deposition process. Thus, the %E of the Zn-Fe-Co alloys will be always less than 100%. The results indicated that the current efficiency of Zn, Co and Fe and Zn-Fe-Co thin coatings decreased with shifting the deposition potential to more cathodic values. Due to the normal co-deposition (part A in Figure 1b) at low cathodic potentials (more positive), the current efficiency of zinc deposited in the deposition potential < -1.0 V is lower than that at > -1.1 V.

4. MECHANISM

According to previous studies conducted during the electrochemical deposition of Zn-Ni-Co alloys on a steel substrate, it has been suggested that the anomalous co-deposition trend observed at higher deposition potentials is due to the formation of zinc hydroxide layer on the steel surface due to increase of HER reaction that suppressed the discharge of most noble metals, e.g. Ni^{2+} and Co^{2+} species [35]. By following this mechanism in a coating bath containing a mixture of zinc, iron, and cobalt species, zinc hydroxide will be deposited first, making a structure rich in Zn than Co and Fe. This is due to the lower solubility product constant (K_{sp}) of $Zn(OH)_2$ (1.2×10^{-17}), which induces its precipitation first compared to $Co(OH)_2$ and $Fe(OH)_3$ which have higher solubility product constants of 1.6×10^{-15}, 8.0×10^{-16}; respectively. By examining the data shown in Table 1 and Fig. 2, it is clear that zinc is the most deposited species, indicating that the results that we obtained from this work are more consistent with this theory. Interestingly, one can also clearly observe that the deposition of cobalt and iron is preferred than zinc at low voltages and vice versa occurred with increased the deposition potentials. The findings indicate that, initially, deposition of Fe^{2+} and Co^{2+} ions, or their monovalent cations intermediates, occurs on the working electrode surface, followed by deposition of Zn^{2+} ions, or its monovalent cation intermediate, on newly deposited CoFe/steel surface, which inhibits the subsequent deposition of Fe and Co, although it does not completely block them. The degree of inhibition depends on the value of the applied voltage since they are directly related to each other.
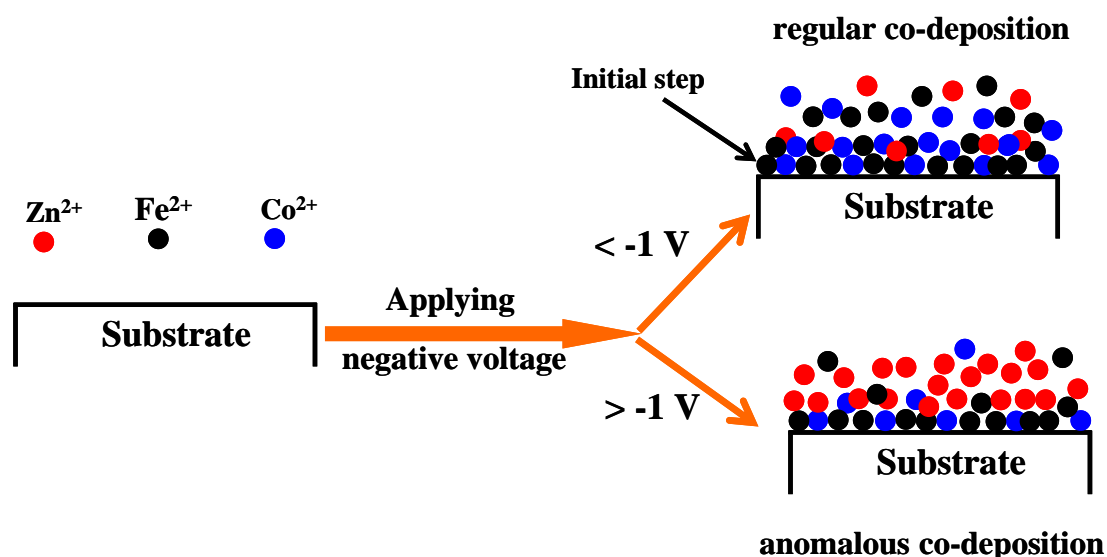

Figure 8. Schematic diagram of the proposed co-deposition mechanism.

Figure 8 illustrates a schematic diagram of the proposed mechanism. Accordingly, the shift in the corrosion potential of coatings deposited using very high deposition voltages (-1.2 to -1.4 V) to more positive values as well as increasing their corrosion resistance can be associated with two important factors: the first is the significant increase in thickness of these alloys ($\approx$ 3.5 µm), and the second is due to selective dissolution of zinc from the deposited thin coatings, leaving behind coatings that are rich in iron and cobalt on the steel surface, and this process is known as dezincification

[30,36,37]. Subsequently, the dissolved Zn^{2+} interacts with OH^- species forming non soluble zinc hydroxide film that passivate the electrode surface.

5. CONCLUSIONS

In this work, the influence of deposition potential on the properties of Zn-Fe-Co alloy coatings has been studied. The results indicated that the change of reduction potentials to more negative values (from -0.6 to -1.0 V) followed by a slight increase in current density indicating the occurrence of regular codeposition process under this conditions. A sharp increase in current density occurred after the coating voltage increased to -1.0 volts, indicating that anomalous co deposition approached. Increased deposition voltages led to a remarkable increase in zinc amounts and contents, contrariwise a decrease in quantities and contents of Co and Fe in the deposits. Coatings with a high content of cobalt up to 37% exhibit superior corrosion resistance. When Zn-Fe-Co is eroded, Zn first begins to dissolve preferably. XRD patterns confirmed that the alloy consist of three different phases. Finally, an adsorption inhibition mechanism has been proposed to explain the observed results.

References

1. P. P. Chung, J. Wang, Y. Durandet, *Friction*, 7(5) (2019) 389-416.
2. S. Sabooni, E. Galinmoghaddam, A. A.Turkin, L. Q. Lu, R. J. Westerwaal, C. Boelsma, E. Zoestbergen, Y. T. Pei, *J. Alloys Compd.*, 836 (2020) 155448.
3. A. Toghan, M. Khodari, F. Steinbach, R. Imbihl, *Thin Solid Thin coatings* 519 (2011) 8139- 8143.
4. M. Marín-Sánchez, E. Gracia-Escosa, A. Conde, C. Palacio, I. García, *Materials,* 11(2018)2035.
5. P. Ferstl, S. Mehl, M. Arman, M. Schuler, A. Toghan, B. Laszlo, Y. Lykhach, O. Brummel, E.Lundgren, J. Knudsen, L. Hammer1, M.A. Schneider, J. Libuda, *J. Phys.l Chem.* C, 119 (29) (2015) 16688-16699
6. F. Faisal, A. Toghan, M. Vorokhta, I. Khalakan, V. Matolin, J. Libuda, *Appl. Surf. Sci.*, 350 (2015) 142-148.
7. A. Toghan, L. M. Rösken, R. Imbihl, *ChemPhysChe*m 11(2010)1452; *Phys Chem Chem Phys.*, 12(2010)9811-9815.
8. S. Sampath, M. Vadivelu, R. Ravindran, P. T. Perumal, V. Velkannan, K. Karthikeyan, *ChemistrySelect*, 5(2020) 2130.
9. M. Heikal, A. Ali, B. S.Ibrahim, A.Toghan, *Constr Build Mater.*, 243 (2020) 118309.
10. M. M. Abou-Krisha, H. M. Rageh, E. A. Matter, *Surf. Coat. Technol.*, 202(15) (2008), 3739-3746
11. T. Boiadjieva-Scherzer, G. Avdeev, T. Vassilev, V. Chakarova, H. Kronberger, M. Monev, M., *Surf Eng.*, 35(2019) 1055.
12. C. Oulmas, S. Mameri, D. Boughrara, A. Kadri, J. Delhalle, Z. Mekhalif, B. Benfedda, Heliyon, 5(2019) e02058.
13. M. M. Abou-Krisha, A. M. Zaky, A. A. Toghan, *Asian J. Biochem.*, 1(2006) 84.

14. Y. T. Hsieh, R. W. Tsai, C. J. Su, L. W. Sun, *J. Phys. Chem*. C, 118(2014) 22347.
15. M. M. Abou-Krisha, F. H. Assaf, A. A. Toghan, Electrodeposition of Zn–Ni alloys from sulfate bath, *J. Solid State Electr*., 11 (2) (2007) 244-252.
16. X. Zhang, R. Liu, R., *In.t J. Energy Res*. 2020. https://doi.org/10.1002/er.5103
17. S. Fashu, R. Khan, *Anti-Corrs Method* M., 66(2019) 66, 45.
18. F. Assaf, M. Abou-Krisha, T. A. Yousef, A. Abushoffa, F. El-Sheref, A. Toghan, *Russ. J. Phys. Chem.,* 94(8) (2020) 1708-1715.
19. R. Solmaz, B. D. Karahan, *Int. J. Mine.r Metall Mater*. 27(2020)74.
20. R. S. Bhat, U. Bhat, A. Hegde, *Anal. Bioana.l Electrochem*., 3(2011)302.
21. J. Cheng, L. Ding, Q. Li, C. Chen, R. Wang, X. Kong, Z. Song, X. Zhao, Y. Niu, *J Appl Electrochem.,* 2020. https://doi.org/10.1007/s10800-020-01405-4
22. G. Tsurtsumia, D. Gogoli, N. Koiava, I. Kakhniashvili, N. Jokhadze, T. Lezhava, N. Nioradze, D. Tatishvili, *IOP Conf. Series: Earth and Environmental Science*, 95(2017)042035.
23. H. Faid, L. Mentar, M. R. Khelladi, A. Azizi, *Surf. Eng*., 33(2017) 529.
24. W. Li, P. Liu, P. K. Liaw, *Mat. Res. Lett*., 6(2018)199.
25. M. M. Abou-Krisha, *Appl. Surf. Sci*., 252(2005)1035.
26. M. G. Hosseini, H. Ashassi-Sorkhabi, H. A. Ghiasvand, *J. Surf. Coat. Technol.*, 202(2008)2897.
27. Z.F.Lodhi, J.M.C.Mol, https://www.sciencedirect.com/science/article/abs/pii/S0257897207004495 - !A. Hovestad, H.Terryn, J.H.W.de Wit, *Surf. Coat. Technol*., 202(2007)84.
28. J.B. Bajat, M.D. Maksimović, G.R. Radović, *J. Serb. Chem. Soc.*, 67(2002)625-634.
29. H. Kazimierczak, https://www.sciencedirect.com/science/article/pii/S0013468620302814 - !Z. Świątek, P. Ozg, *Electrochim. Acta*, 338(2020)135889.
30. Z. F. Lodhi, J. M. C. Mol, A. Hovestad, L. Hoen-Velterop, H. Terryn, J. H. W. De Wit, *Surf. Coat. Technol.,* 203(2009)1415.
31. T. Kim, Y. Lee, S. Sanyal, Y. Woo, I. Choi, J. Yi, *Appl. Sci*., 10(2020) 423.
32. F. M. Rivas-Esquivel, G. M. Brisard, R. Ortega-Borges, G. Trejo, Y. Meas, *Int. J. Electrochem. Sci*., 12(2017)2026.
33. A. Lasia, Handbook of Fuel Cells, *Fundamentals, Technology and Applications. John Wiley & Sons, Inc*., 2(2010) 416.
34. B. D. Hall, D. Zanchet, D. Ugarte, *J. App.l Crystallogr*., 33(2000)1335.
35. M. M. Abou-Krisha, H. M. Rageh, E. A. Matter, *Surf. Coat. Technol*., 202(2008)3739.
36. J. Choucri, F. Zanotto, V. Grassi, A. Balbo, M. Touhami, I. Mansouri, C. Monticelli, *Metals*, 9(2019)649.
37. M. D. Fazio, A. C. Felici, F. Catalli, C. D. Vito, *Sci. Rep*., 9(2019)12668.